11th ANKARA INTERNATIONAL AEROSPACE CONFERENCE **AIAC-2021-173**
8-10 September 2021 - METU, Ankara TURKEY

WIND FIELD SIMULATION USING ACTUATOR LINE MODEL WITH CLEAN AND ICED BLADE PROFILES

Huseyin C. Onel*
Middle East Technical University
Ankara, Turkey

Ozcan Yirtici†
Osmaniye Korkut Ata University
Osmaniye, Turkey

Ismail H. Tuncer‡
Middle East Technical University
Ankara, Turkey

ABSTRACT

In this study, a horizontal axis wind turbine is modeled using the so called Actuator Line Model *(ALM), where full resolution of the blade boundary layer over turbine blades is not needed and hence computation is cheaper. An ice accretion model is employed to estimate iced blade profiles, on which different sets of aerodynamic force coefficients are obtained to be used in ALM. Clean and iced cases are compared in terms of wind field parameters in the wake region, force distributions along the blades and turbine performance parameters. Mean velocity contour plots, eddy structures and velocity profiles in the wake and turbine power and thrust production are presented. The axial force over the blades are found to be the dominant factor in the wake deficit. Icing affected the wake region and force distribution over the blades in a non-homogeneous fashion.*

INTRODUCTION

In winter, the wind turbines are exposed to heavy atmospheric icing conditions and to maximize energy production from the turbines that operate under icing conditions performance losses need to be predicted. Accurate air flow-turbine blade interaction is important for a good estimation of turbine performance and wake simulation. On the other hand, optimal positioning of turbines on the field depends on the proper wake calculation, since wake deficit is the primary cause of power loss even in ideal operation conditions. Considering length scales of blade boundary layer and wake propagation are $10^{-3}m$ and $10^{3}m$ respectively, wind farm design becomes a challenging numerical problem where those wide range of length and time scales need to be resolved. Actuator Line Model (ALM) adopts a computationally cheaper approach, where boundary layer resolution (hence dramatic increase in grid size) is avoided. Blades are introduced into the flow domain as virtual lines, consisting of a predefined number of 'blade elements', which acts as moving body force sources.

*Researcher in Aerospace Engineering Department, Email: honel@ae.metu.edu.tr
†Asst. Prof. in Computer Engineering, Email: ozcanyirtici@osmaniye.edu.tr
‡Prof. in Aerospace Engineering Department, Email: ismail.h.tuncer@ae.metu.edu.tr

In this study, ALM's trade-off between inexpensiveness and loss of accuracy is examined by comparing its results to other numerical and experimental data, as well as results proposed by other researchers. As the next step, loosely coupled ice accretion prediction tool is used with this model to predict the ice shapes on NREL 5MW wind turbine and, to estimate the energy looses due to icing.

METHODOLOGY

All results are obtained with numerical methods in a parallel computational environment. `OpenFOAM` is used for the mesh generation and flow solutions. Turbines are represented using the Actuator Line Model (ALM) via the `turbinesfoam` library. Aerodynamic coefficients data for the ALM is obtained with XFOIL using viscous integral boundary layer theory for both iced and clean blades. The ice accretion calculations are performed by using ice prediction tool.

Flow solver, `OpenFOAM` **:**

`OpenFOAM` is an open source CFD code which has various customizable flow solvers as well as preprocessing (`blockMesh` and `snappyHexMesh` are used for mesh generation) and postprocessing (`paraFoam - ParaView` are used for visualization) utilities. It employs finite volume approach in spatial discretization and is capable of running in parallel. Incompressible and unsteady flow solver `pimpleFoam` is used, which is a combination of PISO (*Pressure Implicit with Splitting of Operator*) and SIMPLE (*Semi-Implicit Method for Pressure-Linked Equations*) algorithms Barton [1998]. In this study, transient, incompressible Navier-Stokes equations are solved with Large Eddy Simulation (Smagorinsky SGS) turbulence model:

$$\nabla \cdot \mathbf{u} = 0 \tag{1}$$

$$\frac{\partial \mathbf{u}}{\partial t} + \nabla \cdot (\mathbf{u}\mathbf{u}) = -\nabla p + \nabla \cdot (\nu \nabla \mathbf{u}) + \mathbf{f} \tag{2}$$

where $\mathbf{u}$: velocity vector, p: pressure per density, ν: kinematic viscosity and f is the body force per density per volume. `OpenFOAM` is used for mesh generation and solution. Actuator Line Model (ALM) is implemented by use of `turbinesfoam` library. NREL's 5MW horizontal axis wind turbine (HAWT) has been chosen as the sample turbine.

Actuator Line Model (ALM) and `turbinesfoam` **:**

In ALM, wind turbine blades are introduced into the flow field not as solid boundaries in the classical sense, but as virtual lines which has calculated lift-drag forces distributed along them Sorensen and Shen [2002]. Blades are divided into a number of elements of constant sections. Each element has its airfoil section, chord, span and twist. A local 2D Lift-Drag calculation is done on each element by use of relative velocity and angle of attack at the quarter chord position, which are calculated iteratively at each time step. Resultant force calculated at the mid-span is then distributed among the cell centers in the vicinity, via $\mathbf{f}$ term in (2). Distribution is in the form of a normal distribution to prevent singular unstable behavior. This functionality is implemented by `turbinesfoam` , which is an ALM extension library for `OpenFOAM` Bachant et al. [2019].

Ice accretion prediction tool:

Ice accretion prediction involves complex physics comprising aerodynamics, heat transfer and multi-phase flow, which are all time-dependent and involve geometric deformation. The method employed here iteratively predicts the ice accretion on aerodynamic surfaces as a result of water droplets impacting the blade surface. It employs the general methodology for the simulation of ice accretion on airfoils, which is based on the successive calculation of air flow, water droplet trajectories, collection efficiency, heat transfer balance and accreted ice. Detailed information and more validations can be found about ice accretion predictions in Yirtici et al. [2019a,b].

RESULTS

First, the ice accretion model was employed to estimate the ice shapes over blade sections. Then, the aerodynamic coefficients are calculated for both clean and iced profiles. After obtaining the coefficients, the Actuator Line Model (ALM) was employed to observe the turbine and wake characteristics. Two separate cases, that are for clean and iced blade profiles, are simulated. Distribution of parameters along the blades, turbine power production and the variations of flow variables in the wake region for these two cases are presented.

Solution grid and boundary conditions

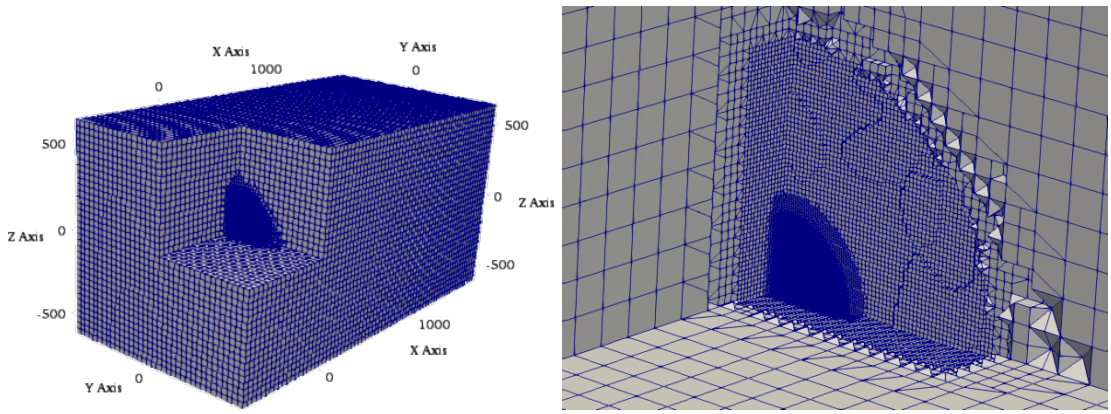

Figure 1: Mesh, clipped (left) and rotor region zoomed (right)

The mesh consists of a single rectangular block with regions of various refinement levels. The turbine is located at the origin $< 0, 0, 0 >$ and the domain span is $(-3D, 10D)$ in x-direction and $(-3D, 3D)$ in y and z-directions. Inflow speed is uniformly $U_\infty = 10\ m/s$ without any atmospheric turbulence. The ground has not been modeled, instead, the turbine is located at the middle of the domain, such that it is free of any form of boundary effects. Free stream conditions are applied at the lateral boundaries. Zero gradient boundary conditions are applied for all field variables at the outlet. The grid is gradually refined from $\Delta_g = 63m$ at farfield to $\Delta_g = 1.97m$ at the rotor region (corresponding to 32 cells per turbine radius) (Figure 1), where Δ_g denotes the uniform cell size. This region of maximum refinement extends from $-1D$ upstream to $8D$ downstream of the turbine, spanning throughout the whole wake region of interest for taking measurements.

The model turbine, NREL-5MW

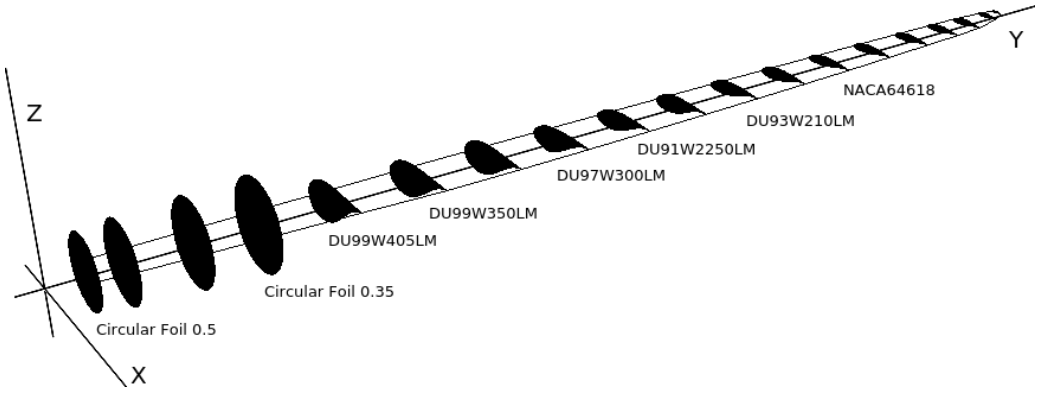

Figure 2: NREL-5MW blade geometry and airfoil sections

The NREL-5MW horizontal-axis wind turbine is selected as the model turbine. It is $126m$ in diameter and has 3 blades. All simulations has been run for tip speed ratio $TSR = U_{tip}/U_\infty = 8$, which corresponds to $12.1\ RPM$. The turbine geometry is defined at 19 radial positions with 2 circular and 6 airfoil profiles 2.

Ice accretion predictions on NREL 5MW wind turbine

Blade profiles	DU 40, DU 25, DU 21, NACA 64618 × 2 (Sec. A-E)
Rotational speed	12.1 rpm
Rated speed	11.4 $m.s^{-1}$
Root chord	4.557 m
Tip chord	1.419 m
Turbine diameter ,R	63 m
Twist	13.308 degrees (max.)

Table 1: Properties of NREL $5mW$ wind turbine.

Ice shape prediction is performed along the large scale NREL 5MW wind turbine blade for five different airfoil profiles (Table 1) along its span under slight rime ice conditions. The predicted rime ice profiles along the span are shown in Figure 3. It is clearly seen that the ice accumulation increases from midspan to tip along the spanwise direction. This is expected result since the sectional chord length is decreasing and sectional velocity is increasing from root to tip. These predicted ice shapes will be used to create iced blade turbine to compare power loss due to icing.

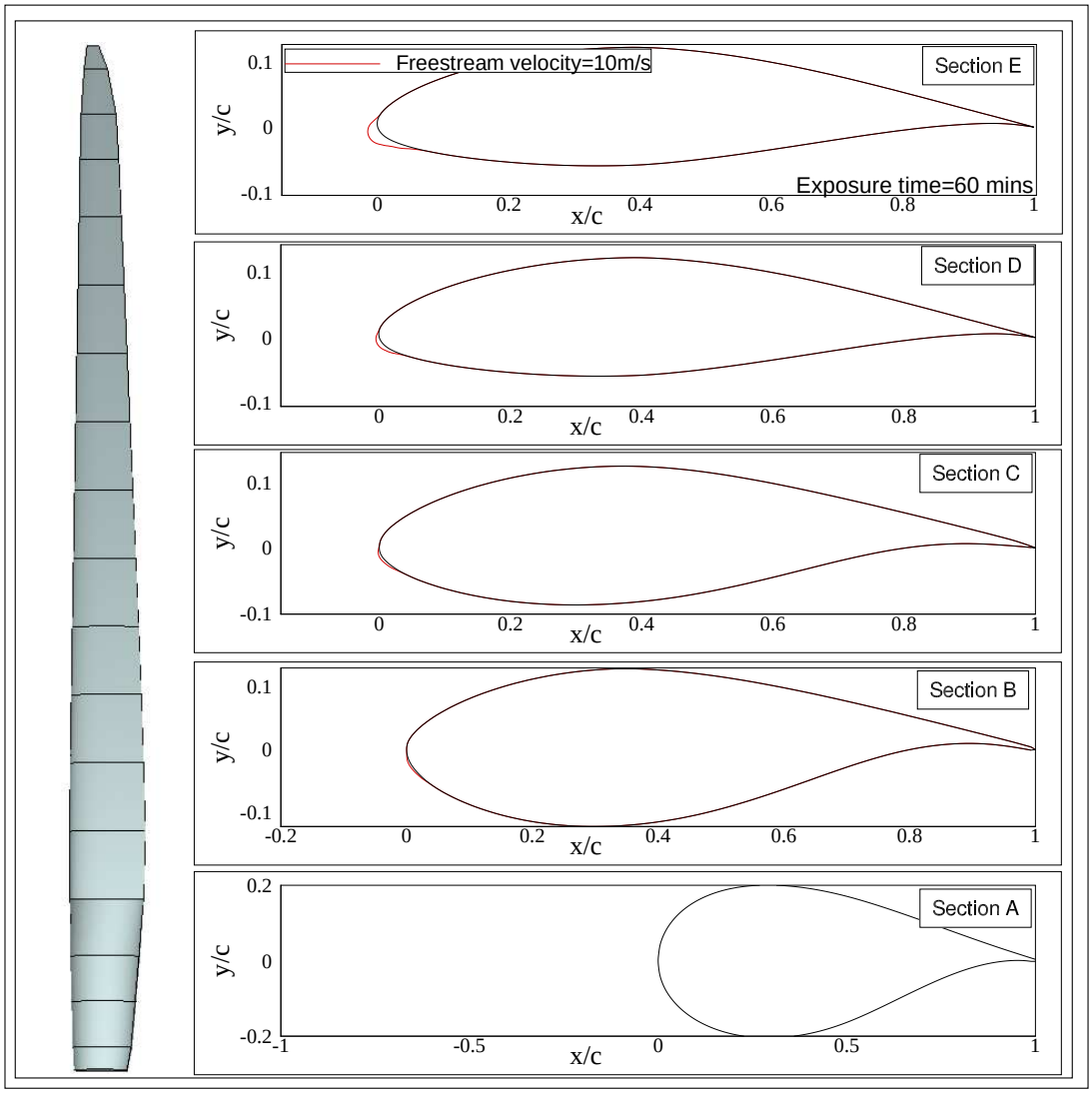

Figure 3: Iced turbine blade profiles (LWC=0.2 g/m^3, MVD=20μm,T_a=-10 °C).

Investigation of the wake region

The region of interest is the $-1D < x < 7D$ region. One rotation of the turbine takes $4.95s$. The simulation was run for a total duration of $t_f = 200s$ (≈ 40 rotations). Velocity field was averaged over the last $50s$ of the simulation ($150s < t < 200s$), corresponding to ≈ 10 rotations, to obtain mean velocities ($\bar{U}$).

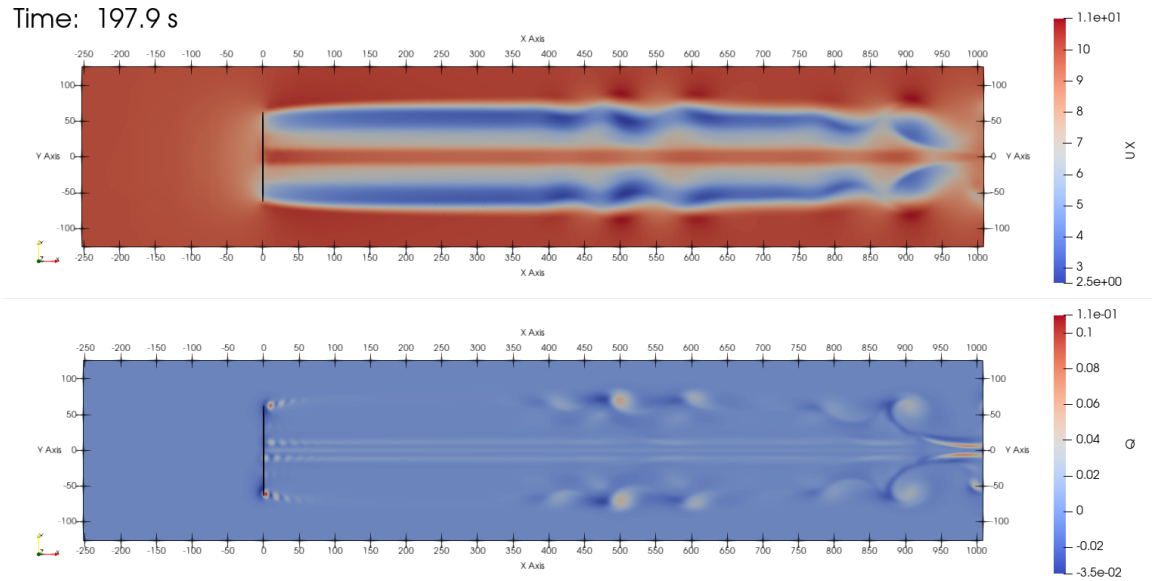

Figure 4: Instantaneous axial velocity U_x (top) and Q (bottom) contours of the clean case (solid black line indicates the turbine location virtually).

The mid-plane contours of instantaneous velocity and Q for the clean case are presented in Figure 4. The figure shows the latest output ($t = 197.9s$). Strongest and most concentrated eddies can be seen emanating from the blade tips, which gradually dissipate within the first $1D$ downstream. Larger eddies with smaller core strength can also be seen further downstream, which are observed to be formed, travel and get dissipated frequently throughout the simulation. These contours are found to be almost indistinguishably similar for both clean and iced cases in terms of a qualitative assessment. Hence, another contour plot is generated that shows the difference of the mean axial velocity between clean and iced cases ($\bar{U}_x^{\text{diff.}} = \bar{U}_x^{\text{iced}} - \bar{U}_x^{\text{clean}}$) (Figure 5).

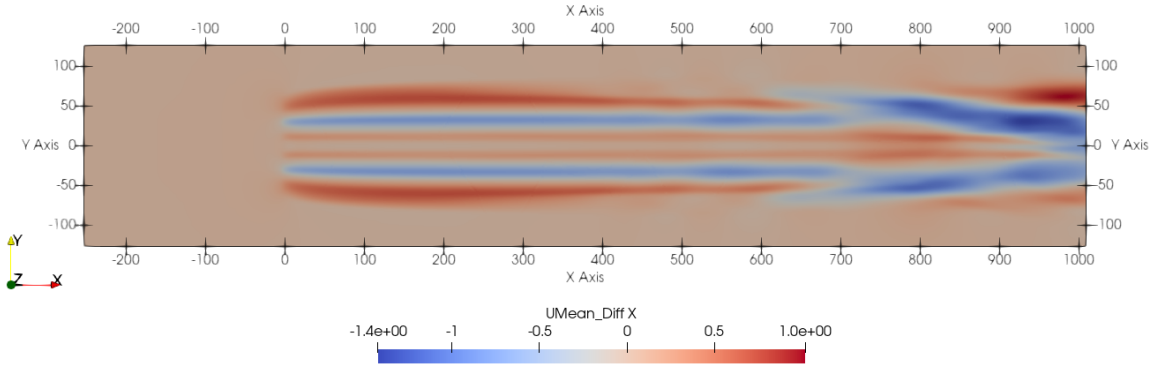

Figure 5: Difference of mean axial velocity between clean and iced cases ($\bar{U}_x^{\text{diff.}} = \bar{U}_x^{\text{iced}} - \bar{U}_x^{\text{clean}}$)

Magnitude of the axial velocity component is of interest in the sense that it is the main contributor to the power production by a HAWT's design. Thus, it is important to evaluated for possible downstream turbines that would fall in another one's wake. The mean axial velocity difference between clean and iced cases varies both in the axial and radial directions (Figure 5). The change

in the axial direction is most prominent around the $x \approx 650m \approx 5D$ downstream location. Up to this point in the wake, the wake of the iced turbine blades has a higher flow energy (higher axial velocity) towards the blade tips and vice-versa in the mid-blade region. Past the $\approx 5D$ downstream point, iced case has less axial velocity overall in the radial direction.

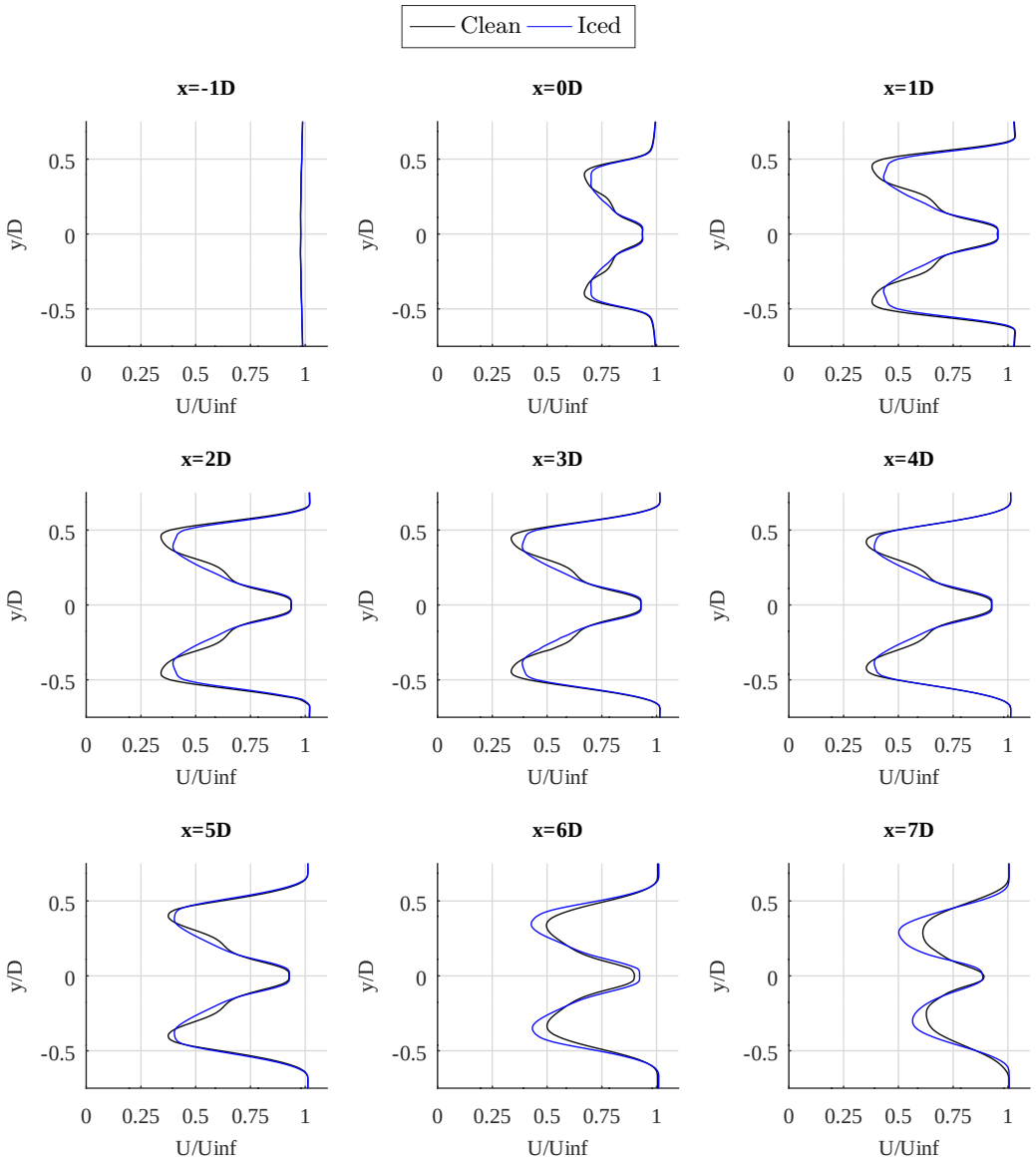

Figure 6: Normalized mean axial velocity profiles ($\bar{U}_x/U_\infty$) plotted along the horizontal lines (y direction) within the wake region.

To see these differences in more detail, velocity profiles are extracted along horizontal lines (along y direction) within the wake region with intervals of $1D$ distance (Figure 6). In addition, the mean axial velocity is integrated and averaged over a disk of $63m$ radius at the same locations (Figure 7). This gives an idea on the overall *energy deficit* within the wake region, since the available power in the wind is proportional to the cube of the average axial velocity ($P = 0.5\rho A U^3$).

As seen in the velocity profiles (Figure 6), the existence of the turbine has a slight retarding effect even $1D$ upstream; the axial velocity is not completely equal to the freestream velocity. Immediately past the rotor, the difference between clean and iced cases become visible. As discussed in Figure 5, icing causes a lower velocity deficit near the blade tip. However, this behavior is reversed at $r \approx 0.3D$ and the clean blades has a wake with higher axial velocity within the $0D < r < 0.3D$ radial range. Vicinity of the root region is excluded from the discussion, since the profiles are cylindrical and

not subject to icing in these simulations. This trend retains up to $x = 6D$, after which the wake characteristic dramatically changes and the wake of the iced blades exhibits a dramatically higher velocity deficit throughout the whole blade radius. In addition, difference between two cases increases from $x = 6D$ to $x = 7D$.

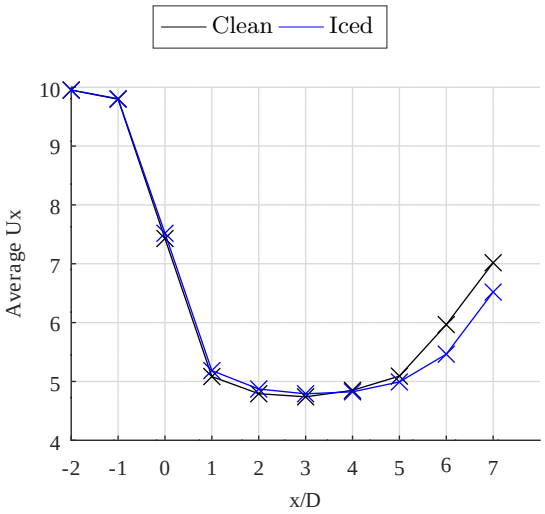

Figure 7: Mean axial velocity averaged over a $63m$ radius disk (rotor swept area) at the wake.

The areal-averaged mean axial velocity plot (Figure 7) shows a trend that supports the previous findings. The available energy in the wind and wake recovery are lower behind the clean blades up to $x = 4D$ downstream position, at which the averaged velocity is almost equal for both cases. This situation indicates that more energy is extracted from the flow by the clean blades. After $x = 4D$ however, the situation reverses and a rapid wake recovery is observed behind the clean blades. At the farthest measurement point of $x = 7D$, average mean velocity of the clean and iced blades are found as $7m/s$ and $6.5m/s$, respectively, corresponding to a significant $\approx 7\%$ difference.

Force and aerodynamic coefficient distributions along the blades

After evaluating the flow field, distributions of forces and aerodynamic coefficients along the blades are investigated (Figure 8). Values shown here are also averaged over the last $50s$ of simulation time (≈ 10 rotations). As expected, lift and drag coefficients ($c_l,\ c_d$) differ significantly throughout the blade span. The most notable difference is that, the c_l value for the iced blades is higher for DU airfoil profiles (up to $r = 0.6R$) whereas it is lower for NACA airfoil profiles. The most remarkable finding is in the force distributions. Relative to the rotor swept disk, the parallel component (torque generating) is noted as tangential (F_t) and the normal component (drag generating) is noted as axial (F_a). Although F_t remains relatively close throughout the span for both iced and clean cases, F_a difference changes direction at $r = 0.6R = 0.3D$. This is in close resemblance with the results discussed in the previous chapter (Figure 6). Noting that F_a is around 1 order of magnitude larger than F_t and its direction is directly opposite to the flow, it is the dominant factor regarding the velocity deficit in the wake. Indeed, the velocity deficit profiles (Figure 6) and axial force distribution (Figure 8) are in agreement in terms of the behavior of the flow along the blade radius and the radial point where this behavior changes. This shows that despite the fact that the overall energy extraction from the flow is higher with the clean blades, it does not necessarily mean that this energy is turned into the power (torque) generation of the turbine.

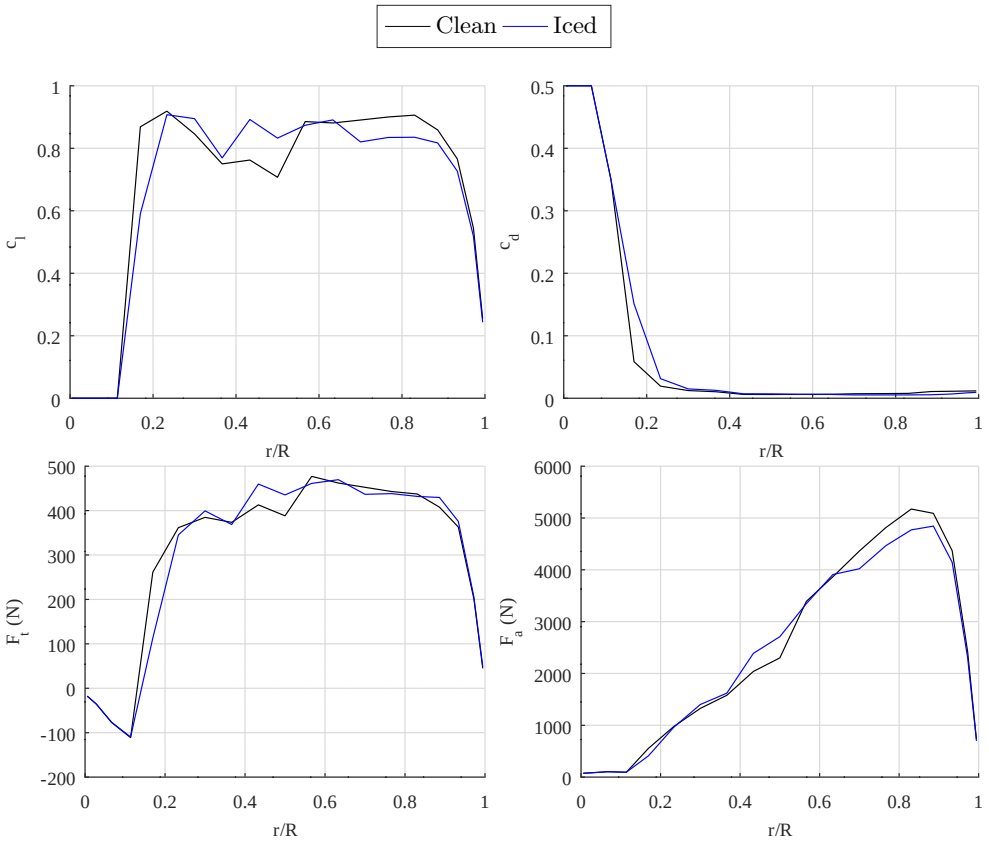

Figure 8: Distribution of aerodynamic coefficients (top) and forces (bottom) over the blades.

Turbine power production

	Clean	Iced
C_P	0.463	0.462 (-0.86%)
C_T	0.753	0.738 (-2%)

Table 2: Power and thrust coefficients of the turbine under clean and iced states.

Finally, power coefficient ($C_P = P/(0.5\rho A U_\infty^3)$) and thrust coefficient ($C_T = T/(0.5\rho A U_\infty^2)$) of both cases are calculated. Compared to the clean blades, the turbine with iced blades generated slightly less power (-0.22%) and less thrust (-2.00%). It is observed that amount of power loss is inconclusively small, and this case is attributed to the using just five different blade sections along the blade under rime ice conditions with fixed Reynolds number.

CONCLUSIONS

An ice accretion model and the Actuator Line Model (ALM) are employed in an uncoupled fashion to compare wind turbines with clean and iced blades. The ice accretion over the blades did not lead to a homogeneous change over the blades or in the wake region. Considering the most torque generating part of the blade ($0.4R < r < 1.0R$) icing did not affect the tangential force significantly. However, icing had an important and non-homogeneous impact on the axial (thrust, drag) force over the blades, which consequently and proportionally affects the velocity deficit in the wage region. Overall power production of the turbine increased slightly, whereas more thrust is generated due to icing. However, power loss could not be captured accurately. Therefore, much additional work will be done to complete this study by performing ice simulations again for more blade sections and with dynamic Reynolds numbers.

References

Bachant, P., Goude, A., daa mec, and Wosnik, M. (2019). turbinesfoam/turbinesfoam: v0.1.1.

Barton, I. E. (1998). Comparison of simple-and piso-type algorithms for transient flows. *International Journal for numerical methods in fluids*, 26(4):459–483.

Sorensen, J. N. and Shen, W. Z. (2002). Numerical modeling of wind turbine wakes. *J. Fluids Eng.*, 124(2):393–399.

Yirtici, O., Cengiz, K., Ozgen, S., and Tuncer, I. H. (2019a). Aerodynamic validation studies on the performance analysis of iced wind turbine blades. *Computers & Fluids*, 192:104271.

Yirtici, O., Ozgen, S., and Tuncer, I. H. (2019b). Predictions of ice formations on wind turbine blades and power production losses due to icing. *Wind Energy*, 22(7):945–958.